CTSS as a novel biomarker for tissue remodeling in CRSwNP: insights from multi-omics research

Chunbo Li[1,2,3,4,#], Yanran Huang[1,2,3,4,#], Jieying Yan[1,2,3,4,#], Yan Yan[3,4,5], Yulin Guo[1,2,3,4], Kexin Li[1,2,3,4], Yihui Wen[1,2,3,4], Jian Li[1,2,3,4], Yi Wei[1,2,3,4,*], Weiping Wen[1,2,3,4,6,*], Zhaofeng Xu[1,2,3,4,*]

Rhinology 64: 4, 0 - 0, 2026
https://doi.org/10.4193/Rhin25.504

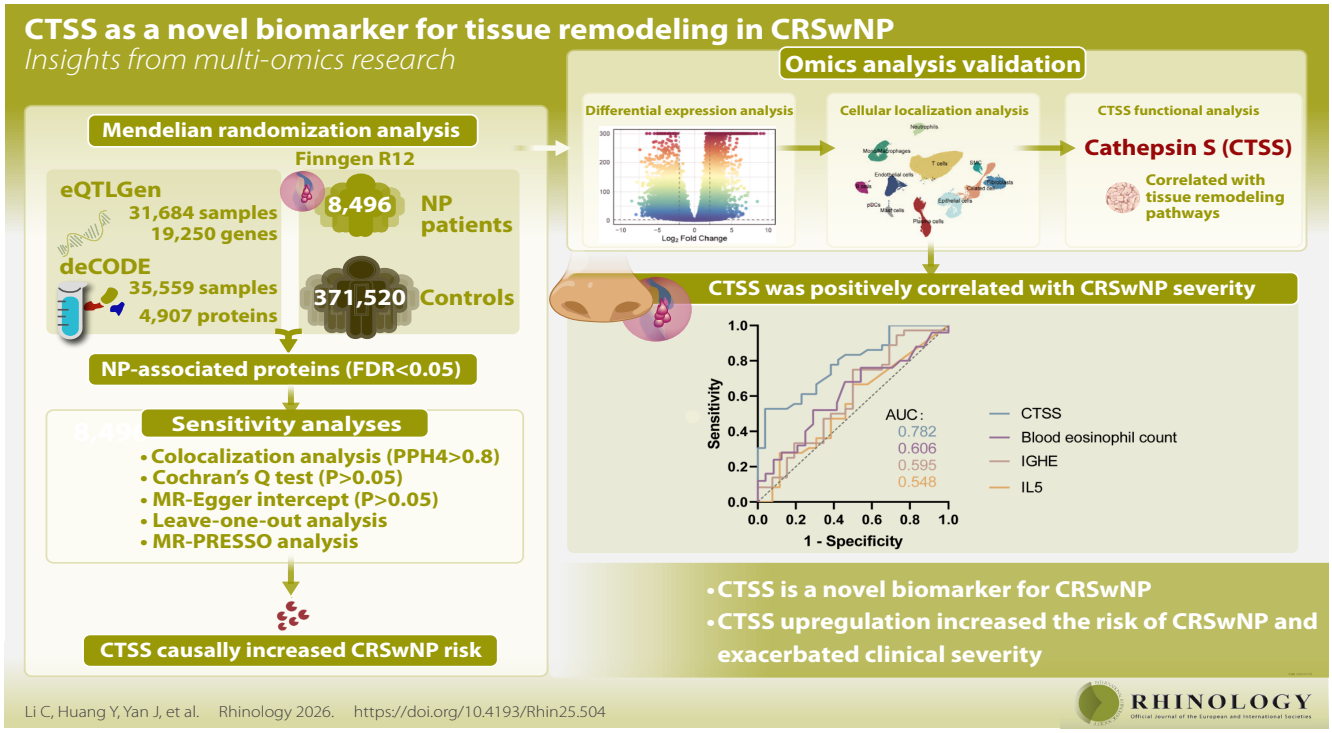

Abstract

Background: Chronic rhinosinusitis with nasal polyps (CRSwNP) is a refractory, relapsing upper airway inflammatory disorder characterized by prominent tissue remodeling. Current therapeutic options remain suboptimal. We aimed to identify novel potential targets and biomarkers using integrative multi-omics.

Methodology: We performed Mendelian randomization (MR) analyses integrating blood expression quantitative trait loci (eQTL) from eQTLGen and plasma protein quantitative trait loci (pQTL) from deCODE with nasal polyps (NP) genome-wide association study data from 8,496 NP patients and 371,520 controls. Significant targets underwent validation via bulk/single-cell RNA sequencing, immunohistochemistry, and immunofluorescence.

Results: MR analyses identified 6 targets causally linked to NP risk in both eQTL and pQTL analyses. Therein, cathepsin S (CTSS) increased the risk of NP, exclusively demonstrating colocalization with NP and exhibiting significant upregulation in NP tissue. Single-cell data showed CTSS mainly express in monocyte/macrophages, and CTSS-high subsets enriched in CRSwNP vs. Control. Immunohistochemistry and immunofluorescence further confirmed high CTSS expression in NP. Moreover, CTSS expression correlated with tissue remodeling pathways and associated with CRSwNP clinical severity.

Conclusions: CTSS may contribute to the pathogenesis of CRSwNP by modulating tissue remodeling. CTSS is a noval biomarker for CRSwNP.

Key words: Mendelian randomization, CTSS, chronic rhinosinusitis with nasal polyps, tissue remodeling

Introduction

Chronic rhinosinusitis (CRS) is characterized by chronic inflammation in the nasal and paranasal sinuses, afflicting over 10% of the global population [1]. Clinically, CRS is stratified into two subtypes based on endoscopic findings: CRS without nasal polyps (CRSsNP) and CRS with nasal polyps (CRSwNP). Approximately 18-20% of CRS patients develop nasal polyps (NP) [2], a subgroup demonstrating frequent asthma comorbidity and predominantly type 2-driven inflammation which is defined by increased mucosal infiltration of Th2 cells, type 2 innate lymphoid cells, and eosinophils, alongside elevated type 2 cytokine levels (IL-4, IL-5, IL-13) [3].

CRSwNP patients often exhibit more severe disease progression, poorer surgical outcomes, higher recurrence rates, and more need for revision surgery [4]. While current biologics targeting type 2 inflammation provide new options for patients, a substantial proportion remain unresponsive and treatment discontinuation often trigger symptom recurrence [5,6]. Moreover, CRSwNP is characterized by prominent tissue remodeling in the nasal mucosa [7], manifesting as edema, histoarchitectural disorganization and enhanced angiogenesis [8]. Tissue remodeling plays a key role in contributing to the poor response to conventional therapies in NP [9, 10]. Currently, there are no biologic agents targeting the tissue remodeling process in nasal polyps, despite pioneering advances in inflammatory bowel disease [11,12]. These persistent therapeutic challenges underscore the critical need to better understand disease pathogenesis and develop new therapeutic strategies for CRSwNP.

Mendelian randomization (MR) estimates causal effects between exposures and outcomes by leveraging genetic variants as instrumental variables [13]. This approach approximates the efficacy of randomized controlled trials while minimizing confounding and reverse causation. Recent advances have integrated expression quantitative trait loci (eQTL) and protein quantitative trait loci (pQTL) into MR analyses, enabling causal inference between gene/protein and complex diseases [14]. Furthermore, the development of bulk and single-cell transcriptomics enables a deeper dissection in disease pathogenesis [15]. In this study, we propose combining eQTL/pQTL-MR with bulk and single-cell RNA sequencing to establish a breakthrough framework for identifying novel potential targets and biomarkers in CRSwNP.

Materials and methods

Study design

Figure 1 illustrated the overall study design. We initially performed two-sample MR analyses using publicly available datasets. The eQTLs and pQTLs were leveraged as genetic instruments to estimate causal effects of gene expression and protein abundance in blood on NP. Sensitivity assessments included Cochran's Q test, MR-Egger intercept test, leave one out analysis, MR-PRESSO analysis and Bayesian colocalization. Bulk and single-cell transcriptomic profiling validated the local expression pattern of the identified protein in NP tissues. Spatial distribution of identified proteins was further confirmed by immunohistochemistry and immunofluorescence assays. Further, potential biological function and clinical value of the target were explored.

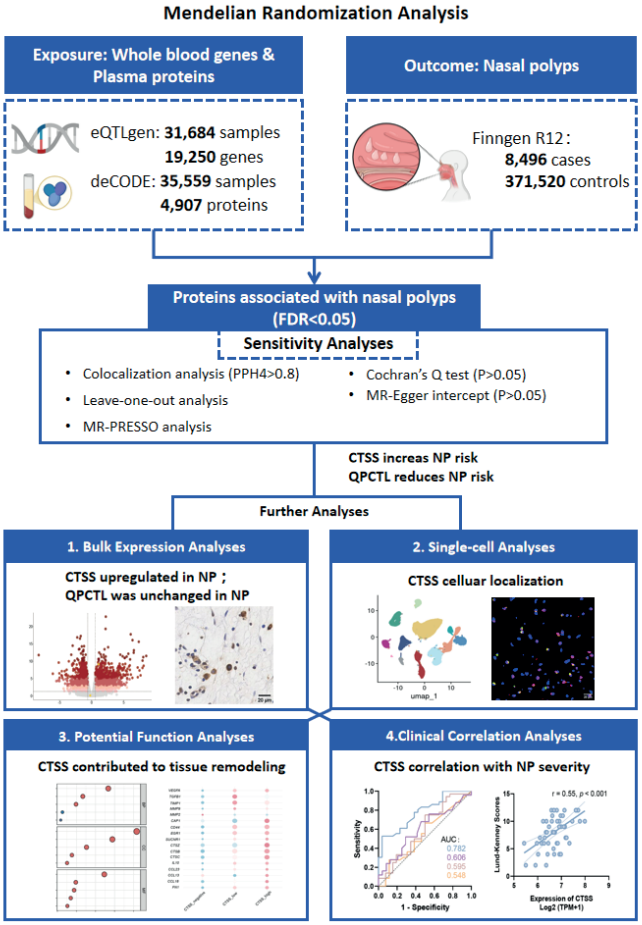

Figure 1. Overview of the study design.

Data source for Mendelian randomization analysis

Blood eQTL data were obtained from the eQTLGen Consortium (https://eqtlgen.org/) which contains 16,989 genes from 31,684 healthy European participants. Comprehensive description can be found in the original publication [16]. Plasma pQTL data originated from deCODE study that quantified the abundance of 4,907 plasma proteins in 35,559 Icelanders based on SomaScan platform [17]. To mitigate the risk of horizontal pleiotropy, cis-pQTLs or cis-eQTLs (SNPs located within a 1,000 kb window from the target gene body) were selected as instrumental variables (IVs) for the following analyses. Genome-Wide Association Studies (GWAS) summary statistics of NP was obtained from the Finnish FinnGen Consortium (Release R12), comprising 8,496 European patients and 371,520 controls, with cases rigorously defined by the International Classification of Diseases (ICD-10 J33) code.

Mendelian randomization and sensitivity analysis

The IVs used in MR analyses must meet three assumptions [18]: 1) IVs are strongly associated with the exposure, 2) IVs are independent of any potential confounders between the exposure and the outcome, and 3) IVs have no direct relationship with the outcome. To meet these assumptions, single nucleotide polymorphisms (SNPs) associated with traits at a genome-wide significance threshold of $P < 5\times10^{-8}$ and low linkage disequilibrium ($r^2 < 0.001$) were selected as IVs. Furthermore, we calculated the F-statistic for each IV to estimate the magnitude of bias originating from weak instruments using the following formula [19]:

$$F=\frac{R^2(N-k-1)}{k(1-R^2)}$$

R^2 reflects the proportion of variance explained by exposure generated via the equation [20]:

$$R^2=\frac{2\times(1-MAF)\times MAF\times\beta^2}{SE^2\times N}$$

where N is the sample size of the exposure, MAF is the minor allele frequency of the SNP, and beta is the estimated genetic effect on exposure. We exclusively maintained those IVs with an F-statistic > 10 to avoid biases engendered by weak IVs [19]. To avoid the influence of confounders, we ascertained and excluded SNPs that were linked to potential confounders in the PhenoScanner GWAS database (http://www.phenoscanner.medschl.cam.ac.uk/). In addition, we excluded the SNPs closely related to the outcome to satisfy the assumption that IVs are related to the outcome only through exposure.

When only one SNP was available as the IV, we performed MR analyses using the Wald ratio method. For analyses with ≥2 IVs, we applied five complementary approaches: inverse-variance weighted (IVW), MR-Egger, weighted median, simple mode, and weighted mode. The IVW method served as our primary estimator due to its superior robustness [21]. The Benjamini-Hochberg procedure was performed for multiple testing. FDR<0.05 was considered significant.

For sensitivity analyses, MR-Egger intercept was conducted to detect horizontal pleiotropy [22], Cochran's Q test for heterogeneity and MR-PRESSO for outliers and pleiotropy [23]. Leave-one-out analyse was used to check if individual SNPs drove significant results [24]. Furthermore, candidate proteins exhibiting significant causal effects on NP risk in both eQTL and pQTL MR analyses were subjected to colocalization testing using the R package "COLOC" (v5.2.3) [25]. This step assessed whether protein-NP associations shared causal genetic variants. The analyses offered posterior probability for each hypothesis tested [26]: H0: No association with either trait; H1: Association with trait 1 only; H2: Association with trait 2 only; H3: Association with both traits (independent causal variants); H4: Association with both traits (shared causal variant). Posterior probability of H4 (PPH4) ≥ 0.80 was considered as strong evidence for colocalization and gave further support of MR result [26].

Bulk RNA sequencing data and analysis

The bulk RNA sequence samples were sourced from the Department of Otorhinolaryngology at Sun Yat-sen University First Affiliated Hospital, including 15 nasal mucosal tissues from healthy controls (HC), 18 sinus mucosal tissues from CRSsNP patients, and 62 NP tissues from CRSwNP patients. Additional enrollment details are provided in the Supplementary materials. Total RNA was isolated from snap-frozen tissues using the RNeasy Mini Kit (QIAGEN, Germany), followed by cDNA synthesis with the iScript cDNA Synthesis Kit (Bio-Rad, USA). Raw paired-end sequencing data quality was assessed via MultiQC. Differential expression analyse was performed using DESeq2 (v1.34.0) with Wald tests. P-values were adjusted for multiple testing via the Benjamini-Hochberg procedure. Genes meeting thresholds of log2FoldChange ≥ 0.585 and adjusted $P < 0.05$ were defined as differentially expressed, consistent with previous publications [27-29].

Single-cell sequencing data and analysis

Single-cell RNA sequencing analyse utilized the publicly available dataset HRA000772 (accession: https://ngdc.cncb.ac.cn/gsa-human), with data usage authorized by the originating institution. The cohort included 5 HCs, 5 CRSsNP, and 11 CRSwNP. Raw sequencing data underwent initial processing through Cell Ranger (v7.0.0) to generate gene expression matrices. Subsequent analyses were conducted mainly using Seurat (v5.2.1) and: Harmony (v1.2.3). After quality control excluding cells with <200 or >4,500 detected genes and >15% mitochondrial gene content, data were normalized via log-normalization. Harmony corrected batch effects across samples, and dimensionality reduction was performed using PCA followed by UMAP/t-SNE projection.

Immunohistochemistry and immunofluorescence staining

Paraffin sections from 10 HC, 10 CRSsNP, and 10 CRSwNP cases underwent standard deparaffinization, rehydration, heat-induced antigen retrieval (sodium citrate, pH 6.0) and blocking with 10% goat serum. Sections were incubated with rabbit anti-human CTSS antibody (1:200; Affinity Biosciences; DF8246) at 4°C overnight, followed by Dako EnVision FLEX/HRP detection system (K5007). Five randomly selected 400× fields per sample were analyzed using ImageJ (v 1.54f) to quantify positive cell ratio (positive cells/total cells × 100%).

Paraffin sections from 8 HC, 8 CRSsNP, and 8 CRSwNP cases underwent standard deparaffinization, rehydration, antigen retrieval (sodium citrate, pH 6.0), permeabilization (0.3% Triton X-100), and blocking with 10% goat serum. Sections were co-incubated overnight at 4°C with rabbit anti-human CTSS (1:200; Affinity Biosciences; DF8246) and mouse anti-human CD68 (1μg/ml; Abcam; ab201340), followed by 30-min room temperature incubation with Alexa Fluor 488 goat anti-mouse IgG (H+L) (1:500; Thermo) and Alexa Fluor 594 goat anti-rabbit IgG (H+L)

(1:500; Thermo). The proportion of $CTSS^+CD68^+$ cells among $CD68^+$ cells was quantified in five random 400× fields/sample using ImageJ (v 1.54f).

Statistical analysis

Statistical analyses were performed using the Prism GraphPad version 8. Comparisons between two groups were performed by Mann-Whitney U test. Differences among multiple groups were assessed by Kruskal Wallis test followed by a multiple comparison test. Correlations between two variables were performed by Spearman correlation test. P values less than 0.05 were considered significant (*P < 0.05, **P < 0.01, ***P < 0.001 and ****P < 0.0001).

Results

Mendelian randomization analysis

In our MR analyses, 189,986 cis-eQTLs for 13,698 genes from the eQTLGen consortium were used as IVs and NP as the outcome to estimate the causal effect of genes expression in blood on NP. 884 genes were potentially causally associated with NP at FDR<0.05 (Figure 2A). At the proteomic level, we identified 3,664 cis-pQTLs corresponding to 1,326 plasma proteins from an initial set of 4,907 candidates for MR analyses. 12 plasma proteins exhibited causal associations with NP at FDR<0.05 (Figure 2A). Integrating eQTL and pQTL MR results, we finally identified 6 proteins demonstrating causal associations with NP (Figure 2A-B; Table S2). Among which 5 exhibited consistent causal effect directions on NP in both eQTL and pQTL analyses (IL2RB exhibits opposite causal effects on NP in eQTL versus pQTL analyses), including 1 risk factor—Cathepsin S (CTSS) and 4 protective factors (B3GALT6, QPCTL, LEAP2, GLB1). To determine whether the causal relationships between the identified circulating proteins and NP shared common genetic variants, we performed colocalization analyses and CTSS (PPH4=0.996) and QPCTL (PPH4=0.935) showed robust evidence for colocalization with NP (Figure 2C-D). Furthermore, no heterogeneity (Cochran's Q test, P > 0.05) and pleiotropy (MR-Egger intercept, P > 0.05; Global test, P > 0.05) were observed for the MR results of CTSS and QPCTL (Table S3). No single SNP had a significant impact on the MR results of CTSS and QPCTL (Figure S1).

High expression of CTSS in monocyte/macrophages in nasal polyps

To further verify the potential targets screened by MR analyses, we employed bulk RNA-sequencing to further examined the expression of CTSS and QPCTL in nasal tissue. As shown in Figure 3A-C, differential analyses revealed significant upregulation of CTSS in CRSwNP compared to HC (Log2FoldChange = 1.102, $P = 7.093E^{-10}$), while CRSsNP exhibited no significant elevation relative to HC (Log2FoldChange = 0.570, P =0.020). Conversely, QPCTL expression remained stable among subgroups without significant variation (CRSwNP vs. HC: Log2FoldChange = -0.202, P =0.723; CRSsNP vs. HC: Log2FoldChange = -0.089, P =0.922). Immunohistochemical staining also revealed that the proportion of CTSS-positive cells was significantly higher in the tissues of CRSwNP compared to both HC and CRSsNP (Figure 3D-E). Furthermore, to understand the cellular origin of CTSS in nasal mucosa, we performed single-cell RNA sequencing analyses. After stringent quality control, total 108,244 cells from 21 samples were retained for analyses. Following batch correction, dimensionality reduction, clustering, and cell type annotation, we identified 12 cell types (Figure 4A-B). Monocyte/macrophages demonstrated the highest CTSS expression burden (Figure 4C), with significantly elevated mean expression in CRSwNP versus controls and CRSsNP (Figure 4D). We further stratified monocyte/macrophages by CTSS expression levels (zero and median cutoff) revealed three subsets: CTSS-negative, CTSS-low and CTSS-high. CTSS-high subsets were enriched in CRSwNP compared to HC (U = 8, P = 0.028) (Figure 4E-F). Additionally, immunofluorescence staining indicated that the proportion of CD68 and CTSS double-positive cells in CRSwNP was significantly higher than in both HC and CRSsNP groups (Figure 4G-H).

Potential biological function of CTSS in CRSwNP

Based on the median intercept value of CTSS expression, we divided the bulk RNA sequencing samples of CRSwNP (62 cases) into high-CTSS-expression and low-CTSS-expression groups. 655 differential expressed genes (557 upregulated and 98 downregulated) were found between high-CTSS-expression group and low-CTSS-expression group. GO and KEGG enrichment analyses revealed that most enriched pathways were associated with tissue remodeling (Figure 5A-B). We also identified a positive correlation between CTSS expression and genes related to tissue remodeling (included epithelial remodeling and extracellular matrix remodeling) (Figure 5C). Single-cell sequencing data also revealed similar findings. Compared to CTSS- monocytes/macrophages, the CTSS+ monocytes/macrophages exhibited upregulated expression of most genes related to tissue remodeling, especially in the high-CTSS group (Figure 5D).

CTSS correlated with CRSwNP severity

Recurrent CRSwNP or comorbid asthma were classified as severe CRSwNP (svCRSwNP)[30], and 36 CRSwNP patients were classified as svCRSwNP. We found that higher CTSS expression was showed in svCRSwNP group compared to normal CRSwNP (Figure 6A). Critically, the performance of predicting svCRSwNP status of CTSS was superior to blood eosinophil counts, IGHE and IL5 expression (Figure 6B). Correlation analyses with clinical severity metrics established positive associations between CTSS expression level and Lund-Kennedy scores, NP scores, unilateral maximal polyp scores, Lund-Mackay scores, and sinonasal symptom VAS scores (Figure 6C).

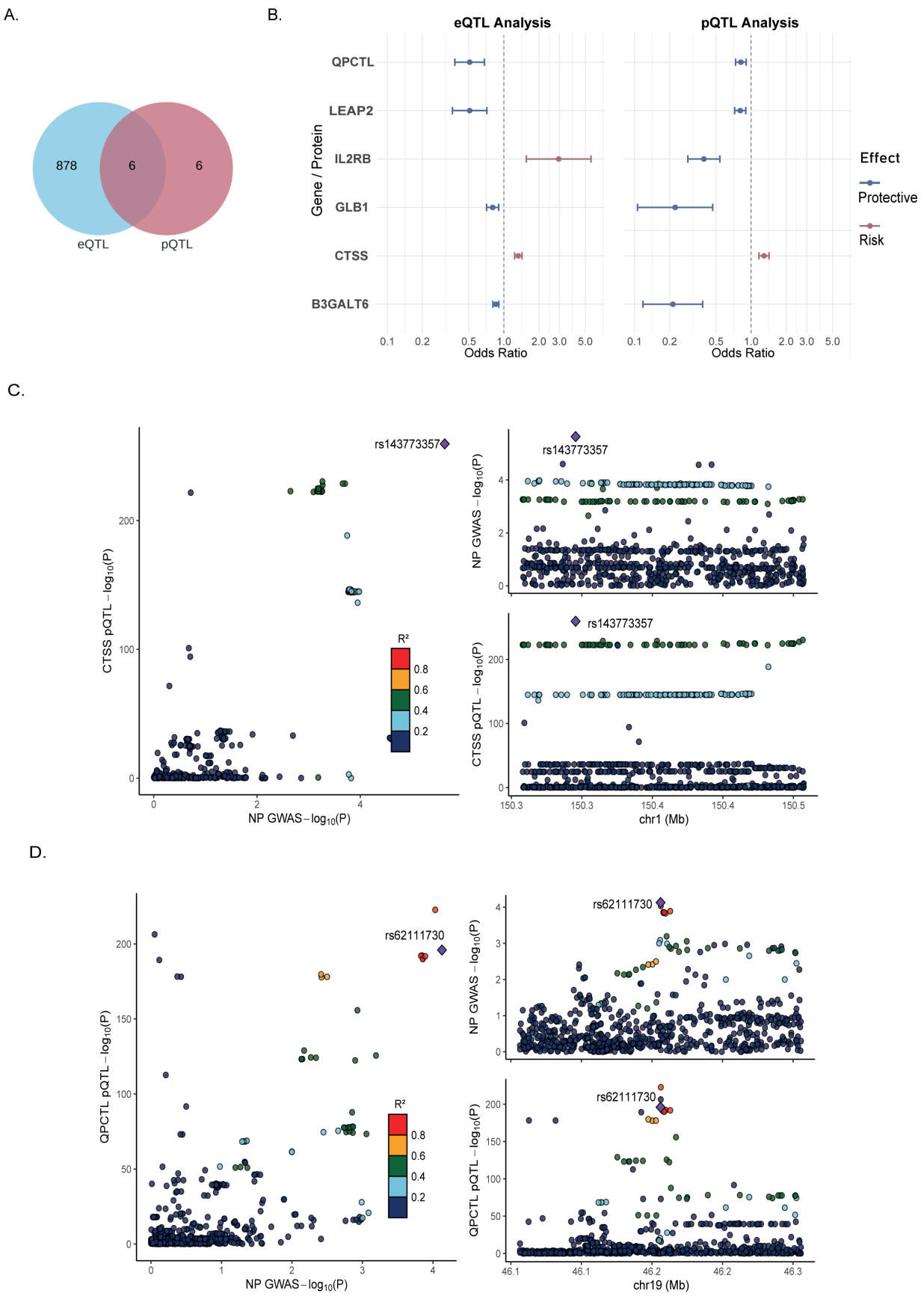

Figure 2. Results of Mendelian randomization analyses. (A) Venn diagram of the rusults for eQTL and pQTL datasets. (B) Forest plots showing the common six potential targets for nasal polyps in eQTL and pQTL datasets. (C) Regional plot of colocalization evidence of CTSS and nasal polyps. (D) Regional plot of colocalization evidence of QPCTL and nasal polyps.

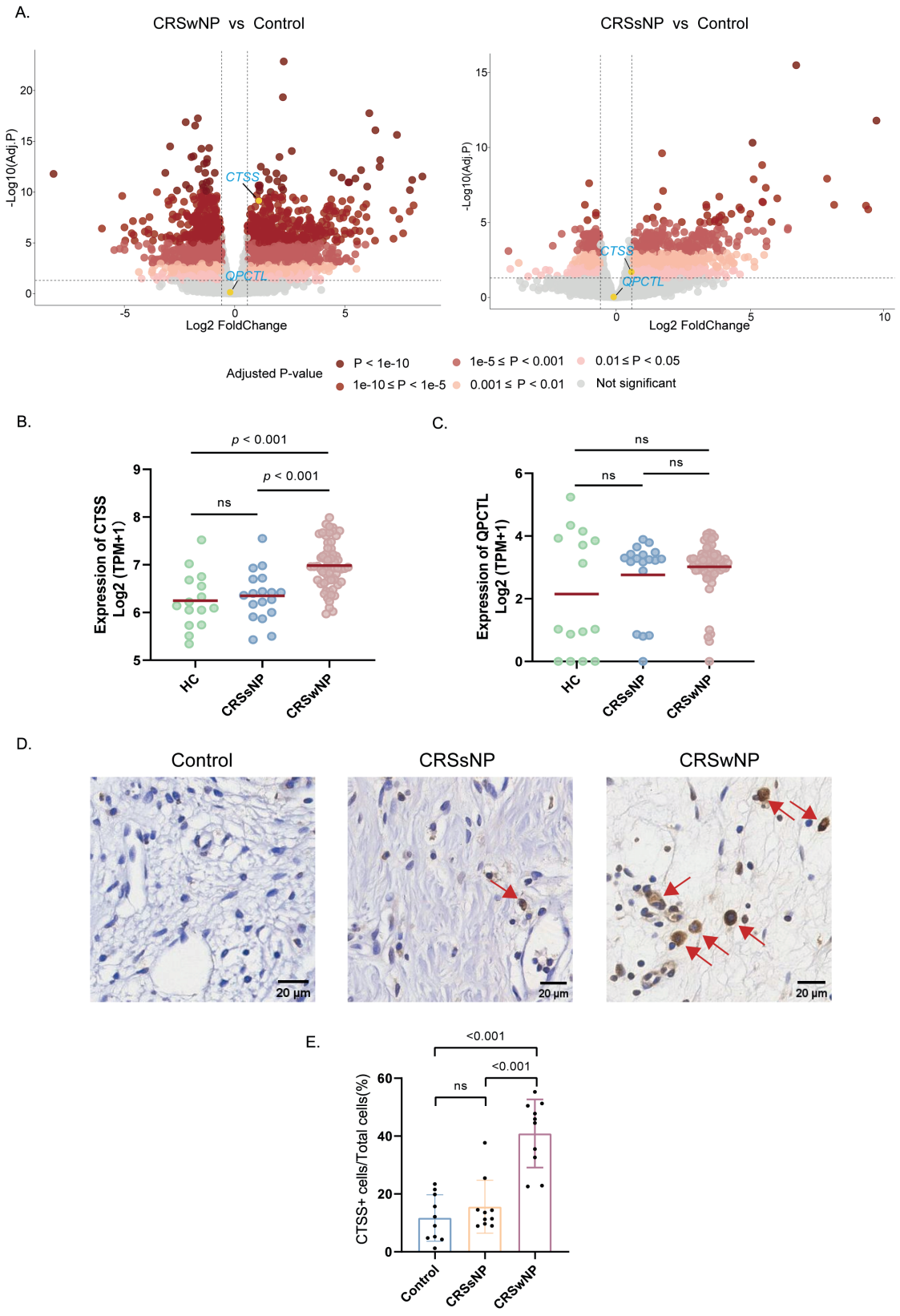

Figure 3. The total expression level of CTSS was increased in nasal polyps. (A) Volcano plots showing the differential expression of CTSS and QPCTL in CRSwNP vs. Control and CRSsNP vs. Control for bulk RNA sequencing. (B-C) The normalised mRNA expression level of CTSS and QPCTL in inferior turbinate of healthy controls (n=15) nasosinusal mucosa of CRSsNP (n=18) and nasal polyps of CRSwNP (n=62) were measured by bulk RNA sequencing. (D-E) Representative immunohistochemical staining and quantitative Analyses of CTSS expression in healthy control (n=10), CRSsNP (n=10) and CRSwNP (n=10) tissues. Scale bar, 20 μm.

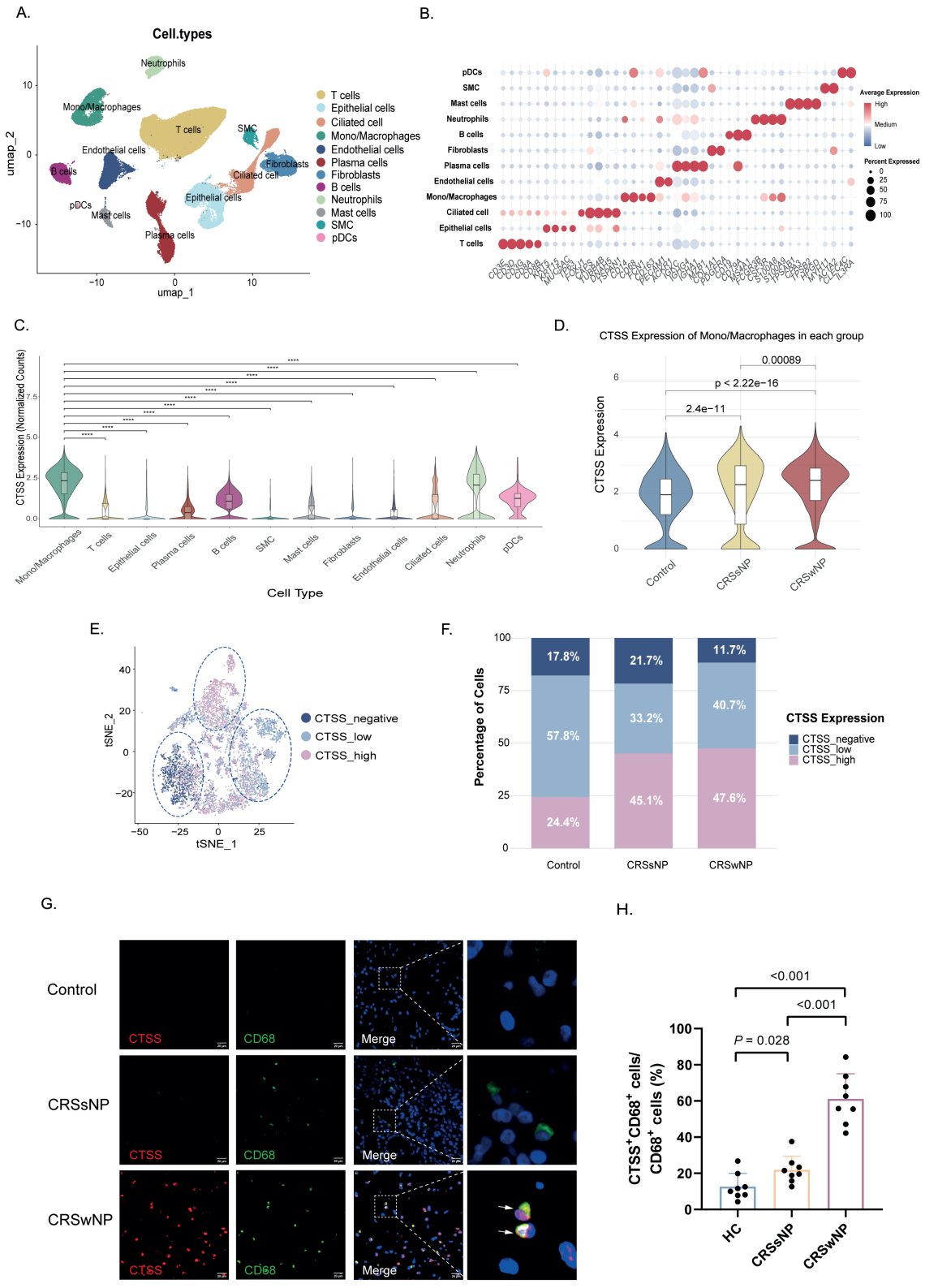

Figure 4. CTSS upregulation primarily localized to mono/macrophages in nasal polyps. (A) UMAP plot displaying 108,244 cells from 21 samples clustered into 12 cell types. (B) Dot plot showing marker genes of each cell type. (C) Violin plot demonstrating significantly higher CTSS expression in mono/macrophages than other cell types. (D) Violin plot showing the CTSS expression levels of mono/macrophages among groups. (E) t-SNE plot of 6,692 mono/macrophages clustering based on CTSS expression. (F) The proportion of CTSS negative/ low-expression/ high-expressed mono/macrophages in each group. (G) Representative immunofluorescent assay showing CTSS (red) colocalized with CD68 (green) in macrophages in CRSwNP (n=8). Scale bar, 20 μm. (H) Percentage of CTSS+ macrophages (CTSS+CD68+) in total macrophages (CD68+) among groups. Mono/Macrophages: monocyte and macrophage subset pDCs: plasmacytoid dendritic cells; SMC: smooth muscle cells. *P< 0.05, **P< 0.01, ***P< 0.001, ****P< 0.0001.

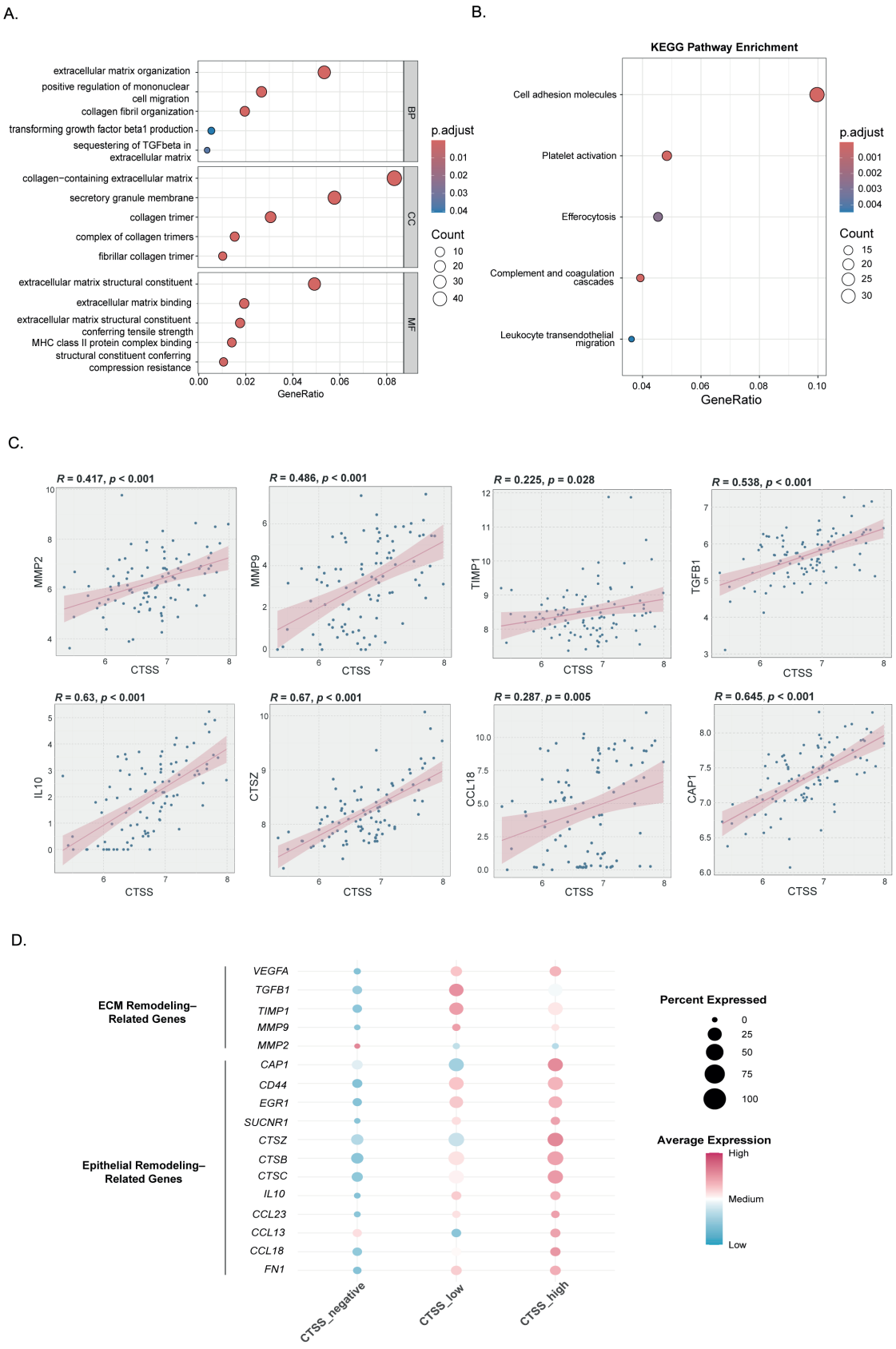

Figure 5. CTSS related to tissue remodeling. (A-B) GO and KEGG enrichment analyses of the differentially expressed genes for CTSS-high CRSwNP vs. CTSS-low CRSwNP. (C) Pearson correlation Analyses between CTSS and ECM remodeling-related genes (MMP2, MMP9, TIMP1 and TGFB1) and epithelial remodeling related genes (IL10, CTSZ, CCL18 and CAP1) based on the normalised expression level measured by bulk RNA sequencing. (D) Dot plots depicting the expression levels of ECM remodeling related genes and epithelial remodeling-related genes among CTSS-negative, CTSS-low and CTSS-high mono/macrophages based on the single-cell data. ECM: extracellular matrix; mono/macrophages: monocyte and macrophage subset.

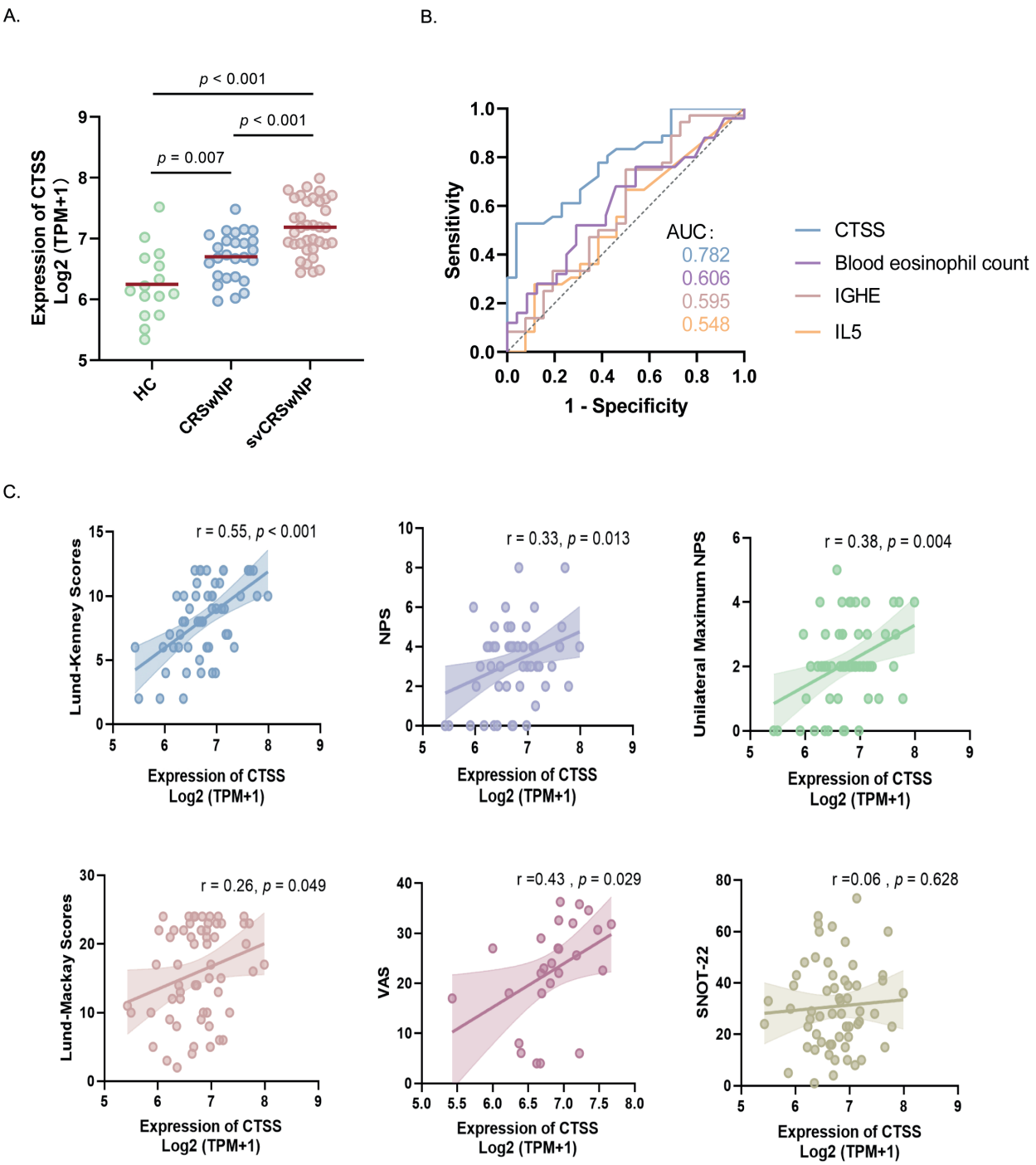

Figure 6. CTSS correlated with the severity of CRSwNP. (A) The normalised mRNA expression level of CTSS in nasal tissue of healthy controls(n=15), CRSwNP patients (n=26) and svCRSwNP patients (n=36). (B) Receiveroperating characteristics curves for predicting svCRSwNP based on CTSS expression level, IL-5 expression level, IGHE expression level (bulk RNA sequencing) and peripheral eosinophil counts in respectively. Areas under the curves are indicated and colour-coded. (C) Pearson correlation Analyses between CTSS expression levels and clinical scores (including Lund-Kennedy scores, NPS, unilateral maximal NPS, Lund-Mackay scores, sinonasal symptom VAS scores and SNOT-22 scores). NPS: nasal polyps scores; SNOT-22: Sinonasal Outcome Test-22.

Discussion

CRSwNP is heterogeneous diseases, exhibiting high postoperative recurrence rates. Although type 2 targeted biologics provide new options for patients, a substantial proportion remain unresponsive. Identifying novel therapeutic targets or biomarkers is still important. For the first time, we integrated eQTL and pQTL data to identify proteins causally associated with NP. We established relationships between 6 plasma proteins and NP

pathogenesis. Among these, only CTSS was validated by colocalization analyses and exhibited upregulated expression in NP. CTSS, which stands for cathepsin S, is a lysosomal cysteine protease belonging to the galactoside histidases family [31]. It is primarily expressed in antigen-presenting cells (such as macrophages) and participates in antigen presentation while regulating multiple inflammatory signaling cascades [31,32]. CTSS has previously been implicated in respiratory inflammatory diseases. Deschamps et al. reported that CTSS knockout or prophylactic pharmacological inhibition reduced plasma IgE level and airway eosinophil infiltration in OVA-challenged mouse model [33]. Zhou et al. demonstrated that Icariside II alleviated airway inflammation and tissue remodeling in mouse asthma models by suppressing CTSS expression [34]. In cystic fibrosis patients, CTSS reduced the lung's defense capacity by degrading protective proteins (such as SLPI and SP-A), thereby promoting pulmonary inflammation and bacterial infections [35,36]. Furthermore, CTSS affected the process of lung fibrosis by degrading extracellular matrix proteins (such as decorin) [37]. These phenomena collectively demonstrate the pivotal role of CTSS in respiratory diseases. Our study showed that CTSS was upregulated in NP and was significantly associated with the severity of NP. These findings bring novel insights for developing new target for CRSwNP. Under specific pathological conditions, CTSS can be secreted extracellularly and retains stable catalytic activity, where it cleaves key extracellular matrix components including elastin, collagen, and fibronectin, to drive tissue remodeling [38]. Zuo et al. demonstrated that macrophage-derived CTSS could promote hepatic fibrosis by cleaving collagen type XVIII alpha-1 chain to generate endostatin, which in turn activates hepatic stellate cells [39]. CTSS also plays a crucial role in left ventricular remodeling after myocardial infarction by regulating TGF-β1 signaling, myofibroblast transdifferentiation, and extracellular matrix protein synthesis [40]. Furthermore, CTSS is associated with tissue remodeling in many respiratory diseases, such as asthma and pulmonary fibrosis [34,41].

Tissue remodeling is prominent in CRSwNP, which plays a pivotal role in the pathogenesis of CRSwNP and likely contributes to the refractory clinical phenotype observed in conventional therapy [9,10]. So far, consensus suggested that the imbalance between matrix metalloproteinases and the tissue inhibitor of metalloproteinases served as a key driver of this process [42]. However, whether CTSS participates in tissue remodeling within NP remains unexplored until now. We demonstrated elevated CTSS expression in NP tissues, with its levels showing a positive correlation with disease severity. Enrichment analyses revealed that differentially expressed genes between CTSS-high and CTSS-low groups were significantly enriched in tissue remodeling-associated signaling pathways. Moreover, CTSS expression exhibited significant positive correlations with both epithelial remodeling-related genes and extracellular matrix remodeling-related genes. These findings suggested that CTSS could modulate the pathogenic progression of CRSwNP through tissue remodeling and exacerbate disease severity. Current management of CRSwNP primarily targets inflammation control and symptom alleviation, with no effective therapeutic options available for modulating tissue remodeling. The identification of CTSS could be potential to bridge this gap.

Furthermore, CTSS could also contribute to the disruption of the epithelial barrier. Chen et al. revealed that macrophage-derived CTSS impairs the blood-brain barrier by cleaving claudin-1, thereby promoting brain aging [43]. Similarly, Yu et al. demonstrated that CTSS compromises the corneal epithelial barrier, facilitating the development of dry eye disease [44]. Furthermore, CTSS was implicated in the disruption of the pulmonary epithelial barrier in chronic obstructive pulmonary disease [45]. Loss of epithelial barrier integrity plays a critical role in the pathogenesis of CRSwNP and serves as one of the initiating events in tissue remodeling [46]. However, it remains unclear whether CTSS is involved in the disruption of nasal mucosal epithelium. Thus, further experimental investigations are warranted to elucidate its potential role to the epithelial barrier of nasal mucosa.

The exploration and identification of novel biomarkers for CRSwNP remains an active area of research. Such efforts are essential to elucidate the mechanisms underlying disease susceptibility, responses to conventional therapies, and postoperative recurrence [47]. We found that CTSS demonstrated superior performance in distinguishing svCRSwNP (recurrent polyps or those comorbid with asthma), compared with the gene expression levels of established risk factors such as IgE, IL-5, and peripheral blood eosinophil counts [48-50]. Furthermore, through MR analysis, we identified 6 plasma proteins causally linked to NP, some of which exhibited protective effects. These proteins provide promising candidates for future biomarker development and therapeutic targeting. Overall, identifying and validating new biomarkers for CRSwNP will deepen the understanding of disease pathophysiology, paving the way for more precise, individualized therapies.

There are certain limitations in our study. Firstly, since the genes covered by eQTLs far exceed the number of protein traits identified in pQTL studies, some potential targets might be overlooked when integrating these two analyses. Secondly, we refrained from filtering eQTL-associated genes for drugability to broaden screening coverage. This approach might increase Type I error risk due to multiple testing, thus we controlled this via Benjamini-Hochberg correction. Thirdly, while utilizing European-derived GWAS summary statistics reduces population stratification bias, our bulk and single-cell transcriptomic data originated from Asian cohorts. Despite consistent analytical trends, this could obscure population-specific effects of CTSS, warranting future validation with multi-ethnic multi-omics datasets. Finally, although the study applied an integrative

multi-omics approach, its retrospective design limits the ability to establish causal relationships regarding the role of CTSS in CRSwNP. Future prospective cohorts combined with experimental mechanistic investigation are warranted to validate these findings.

Conclusion

Our findings suggested that CTSS upregulation increased the risk of CRSwNP, likely by driving tissue remodeling to contribute to the pathogenesis and exacerbate clinical severity. More importantly, this study provided CTSS as a novel biomarker for CRSwNP and pinpointed a direction for future research to identify new therapeutic targets.

Author contributions

CL: conceptualization, data curation, investigation, methodology, writing original draft, visualization. YH: formal analyses, funding acquisition, investigation, validation, writing - review and editing. JY: formal analyses, data curation, visualization, methodology. YY: resources, data curation, visualization. YG, KL, JL: investigation, software. YW: investigation, software, methodology. YW: methodology, writing - review and editing, supervision, project administration. WW: methodology, funding acquisition, writing - review and editing, supervision. ZX: conceptualization, funding acquisition, writing - review and editing, supervision.

Acknowledgments

None.

Conflict of interest

The authors declare no conflicts of interest.

Funding

This study was supported by the National Natural Science Foundation of China (82020108009, 82301282 and 8230127), Guangdong Natural Science Foundation of China (2023B1111040004 and 2023A04J2201), Key Clinical Technique of Guangzhou (2023P-ZD06).

References

1. Sedaghat AR, Kuan EC, Scadding GK. Epidemiology of chronic rhinosinusitis: prevalence and risk factors. J Allergy Clin Immunol Pract 2022, 10(6):1395-1403.
2. Laidlaw TM, Mullol J, Woessner KM, Amin N, Mannent LP. Chronic rhinosinusitis with nasal polyps and asthma. J Allergy Clin Immunol Pract 2021, 9(3):1133-1141.
3. Xu Z, Huang Y, Delemarre T, Cavaliere C, Zhang N, Bachert C. Advances in chronic rhinosinusitis in 2020 and 2021. J Allergy Clin Immunol 2022, 149(3):854-866.
4. Schleimer RP. Immunopathogenesis of chronic rhinosinusitis and nasal polyposis. Annu Rev Pathol 2017, 12:331-357.
5. Cai S, Xu S, Zhao Y, Zhang L. Efficacy and safety of biologics for chronic rhinosinusitis with nasal polyps: a meta-analysis of real-world evidence. Allergy 2025, 80(5):1256-1270.
6. Bachert C, Han JK, Desrosiers M, et al. Efficacy and safety of dupilumab in patients with severe chronic rhinosinusitis with nasal polyps (LIBERTY NP SINUS-24 and LIBERTY NP SINUS-52): results from two multicentre, randomised, double-blind, placebo-controlled, parallel-group phase 3 trials. Lancet 2019, 394(10209):1638-1650.
7. Fokkens WJ, De Corso E, Backer V, et al. EPOS2020/EUFOREA expert opinion on defining disease states and therapeutic goals in CRSwNP. Rhinology 2024, 62(3):287-298.
8. Ahn SH, Oh JT, Kim DH, et al. S100A9 induces tissue remodeling of human nasal epithelium in chronic rhinosinusitis with nasal polyp. Int Forum Allergy Rhinol 2025, 15(2):135-148.
9. Wang X, Sima Y, Zhao Y, et al. Endotypes of chronic rhinosinusitis based on inflammatory and remodeling factors. J Allergy Clin Immunol 2023, 151(2):458-468.
10. Siddiqui S, Bachert C, Bjermer L, et al. Eosinophils and tissue remodeling: relevance to airway disease. J Allergy Clin Immunol 2023, 152(4):841-857.
11. Opdenakker G, Vermeire S, Abu El-Asrar A. How to place the duality of specific MMP-9 inhibition for treatment of inflammatory bowel diseases into clinical opportunities? Front Immunol 2022, 13:983964.
12. Goffin L, Fagagnini S, Vicari A, et al. Anti-MMP-9 antibody: a promising therapeutic strategy for treatment of inflammatory bowel disease complications with fibrosis. Inflamm Bowel Dis 2016, 22(9):2041-2057.
13. Skrivankova VW, Richmond RC, Woolf BAR, et al. Strengthening the reporting of observational studies in epidemiology using Mendelian randomization: the STROBE-MR statement. JAMA 2021, 326(16):1614-1621.
14. Wang S, Yue Y, Wang X, Tan Y, Zhang Q. SCARF2 is a target for chronic obstructive pulmonary disease: Evidence from multi-omics research and cohort validation. Aging Cell 2024, 23(10):e14266.
15. Li X, Wang CY. From bulk, single-cell to spatial RNA sequencing. Int J Oral Sci 2021, 13(1):36.
16. Vosa U, Claringbould A, Westra HJ, et al. Large-scale cis- and trans-eQTL analyses identify thousands of genetic loci and polygenic scores that regulate blood gene expression. Nat Genet 2021, 53(9):1300-1310.
17. Ferkingstad E, Sulem P, Atlason BA, et al. Large-scale integration of the plasma proteome with genetics and disease. Nat Genet 2021, 53(12):1712-1721.
18. Emdin CA, Khera AV, Kathiresan S. Mendelian randomization. JAMA 2017, 318(19):1925-1926.
19. Burgess S, Thompson SG, Collaboration CCG. Avoiding bias from weak instruments in Mendelian randomization studies. Int J Epidemiol 2011, 40(3):755-764.
20. Papadimitriou N, Dimou N, Tsilidis KK, et al. Physical activity and risks of breast and colorectal cancer: a Mendelian randomisation analysis. Nat Commun 2020, 11(1):597.
21. Burgess S, Bowden J, Fall T, Ingelsson E, Thompson SG. Sensitivity Analyses for Robust Causal Inference from Mendelian Randomization Analyses with Multiple Genetic Variants. Epidemiology 2017, 28(1):30-42.
22. Burgess S, Thompson SG. Interpreting findings from Mendelian randomization using the MR-Egger method. Eur J Epidemiol 2017, 32(5):377-389.
23. Verbanck M, Chen CY, Neale B, Do R. Detection of widespread horizontal pleiotropy in causal relationships inferred from Mendelian randomization between complex traits and diseases. Nat Genet 2018, 50(5):693-698.
24. Guan M, Yan L, Li R et al. Integration of leave-one-out method and real-time live cell reporter array system to assess the toxicity of mixtures. Environ Res 2022, 214(Pt 3):114110.
25. Giambartolomei C, Vukcevic D, Schadt EE, et al. Bayesian test for colocalisation between pairs of genetic association studies using summary statistics. PLoS Genet 2014, 10(5):e1004383.

26. Foley CN, Staley JR, Breen PG, et al. A fast and efficient colocalization algorithm for identifying shared genetic risk factors across multiple traits. Nat Commun 2021, 12(1):764.
27. Lv Z, Hu C, Jiang J, et al. Effects of high-dose genistein on the hypothalamic RNA profile and intestinal health of female chicks. J Agric Food Chem 2019, 67(49):13737-13750.
28. Todd JL, Neely ML, Overton R, et al. Peripheral blood proteomic profiling of idiopathic pulmonary fibrosis biomarkers in the multicentre IPF-PRO Registry. Respir Res 2019, 20(1):227.
29. Luo S, Zhao X, Jiang J, et al. Piezo1 specific deletion in macrophage protects the progression of liver fibrosis in mice. Theranostics 2023, 13(15):5418-5434.
30. Lan F, Li J, Miao W, et al. GZMK-expressing CD8(+) T cells promote recurrent airway inflammatory diseases. Nature 2025, 638(8050):490-498.
31. Honey K, Rudensky AY. Lysosomal cysteine proteases regulate antigen presentation. Nat Rev Immunol 2003, 3(6):472-482.
32. Gao H, Zhang Z, Deng J, Song Y. Cathepsin S: molecular mechanisms in inflammatory and immunological processes. Front Immunol 2025, 16:1600206.
33. Deschamps K, Cromlish W, Weicker S, et al. Genetic and pharmacological evaluation of cathepsin s in a mouse model of asthma. Am J Respir Cell Mol Biol 2011, 45(1):81-87.
34. Zhou Y, Huang X, Yu H, et al. TMT-based quantitative proteomics revealed protective efficacy of Icariside II against airway inflammation and remodeling via inhibiting LAMP2, CTSD and CTSS expression in OVA-induced chronic asthma mice. Phytomedicine 2023, 118:154941.
35. Taggart CC, Lowe GJ, Greene CM, et al. Cathepsin B, L, and S cleave and inactivate secretory leucoprotease inhibitor. J Biol Chem 2001, 276(36):33345-33352.
36. Lecaille F, Naudin C, Sage J, et al. Specific cleavage of the lung surfactant protein A by human cathepsin S may impair its antibacterial properties. Int J Biochem Cell Biol 2013, 45(8):1701-1709.
37. Kehlet SN, Bager CL, Willumsen N, et al. Cathepsin-S degraded decorin are elevated in fibrotic lung disorders - development and biological validation of a new serum biomarker. BMC Pulm Med 2017, 17(1):110.
38. Smyth P, Sasiwachirangkul J, Williams R, Scott CJ. Cathepsin S (CTSS) activity in health and disease - A treasure trove of untapped clinical potential. Mol Aspects Med 2022, 88:101106.
39. Zuo T, Xie Q, Liu J, et al. Macrophage-derived cathepsin S remodels the extracellular matrix to promote liver fibrogenesis. Gastroenterology 2023, 165(3):746-761 e716.
40. Chen H, Wang J, Xiang MX, et al. Cathepsin S-mediated fibroblast trans-differentiation contributes to left ventricular remodelling after myocardial infarction. Cardiovasc Res 2013, 100(1):84-94.
41. Yoo Y, Choi E, Kim Y, et al. Therapeutic potential of targeting cathepsin S in pulmonary fibrosis. Biomed Pharmacother 2022, 145:112245.
42. Lygeros S, Danielides G, Grafanaki K, Riga M. Matrix metalloproteinases and chronic rhinosinusitis with nasal polyposis. Unravelling a puzzle through a systematic review. Rhinology 2021, 59(3):245-257.
43. Chen Y, Zhou Y, Bai Y, et al. Macrophage-derived CTSS drives the age-dependent disruption of the blood-CSF barrier. Neuron 2025, 113(7):1082-1097 e1088.
44. Yu Z, Li J, Govindarajan G, et al. Cathepsin S is a novel target for age-related dry eye. Exp Eye Res 2022, 214:108895.
45. Bigot P, Chesseron S, Saidi A, et al. Cleavage of occludin by cigarette smoke-elicited Cathepsin S increases permeability of lung epithelial cells. Antioxidants (Basel) 2022, 12(1).
46. Yan B, Lan F, Li J, Wang C, Zhang L. The mucosal concept in chronic rhinosinusitis: Focus on the epithelial barrier. J Allergy Clin Immunol 2024, 153(5):1206-1214.
47. Staudacher AG, Peters AT, Kato A, Stevens WW. Use of endotypes, phenotypes, and inflammatory markers to guide treatment decisions in chronic rhinosinusitis. Ann Allergy Asthma Immunol 2020, 124(4):318-325.
48. Yu J, Yan B, Shen S, et al. IgE directly affects eosinophil migration in chronic rhinosinusitis with nasal polyps through CCR3 and predicts the efficacy of omalizumab. J Allergy Clin Immunol 2024, 153(2):447-460 e449.
49. Lou H, Zhang N, Bachert C, Zhang L. Highlights of eosinophilic chronic rhinosinusitis with nasal polyps in definition, prognosis, and advancement. Int Forum Allergy Rhinol 2018, 8(11):1218-1225.
50. Wu PW, Huang CC, Chang PH, Lee TJ, Fan YH, Huang CC. Blood eosinophil count is the dominant clinical marker for type 2 inflammatory severity in CRSwNP. Laryngoscope 2025, 135(4):1326-1334.

Yi Wei
E-mail: weiyi6@mail.sysu.edu.cn

Weiping Wen
E-mail: wenwp@mail.sysu.edu.cn

Zhaofeng Xu
E-mail: xuzhaof@mail2.sysu.edu.cn

Chunbo Li[1,2,3,4,#], Yanran Huang[1,2,3,4,#], Jieying Yan[1,2,3,4,#], Yan Yan[3,4,5], Yulin Guo[1,2,3,4], Kexin Li[1,2,3,4], Yihui Wen[1,2,3,4], Jian Li[1,2,3,4], Yi Wei[1,2,3,4,*], Weiping Wen[1,2,3,4,6,*], Zhaofeng Xu[1,2,3,4,*]

[1] Department of Otorhinolaryngology, First Affiliated Hospital of Sun Yat-sen University, Guangzhou, Guangdong, P.R. China

[2] Department of Allergy, First Affiliated Hospital of Sun Yat-sen University, Guangzhou, Guangdong, P.R. China.

[3] Otorhinolaryngology Institute of Sun Yat-sen University, Guangzhou, Guangdong, P.R. China

[4] Guangzhou Key Laboratory of Otorhinolaryngology, Guangzhou, Guangdong, P.R. China

[5] Department of Otolaryngology, the Sixth Affiliated Hospital of Sun Yat-sen University, Guangzhou, Guangdong, P.R. China

[6] Department of Otolaryngology, the Seventh Affiliated Hospital of Sun Yat-sen University, Shenzhen, Guangdong, P.R. China

[#] contributed equally * corresponding authors

Rhinology 64: 4, 0 - 0, 2026
https://doi.org/10.4193/Rhin25.504

Received for publication:
September 8, 2025
Accepted: April 9, 2026

Associate Editor:
Sanna Toppila-Salmi

This manuscript contains online supplementary material

SUPPLEMENTARY MATERIAL

Supplementary Material and Methods

Study participants

The bulk RNA sequence samples and tissue section samples were sourced from the Department of Otorhinolaryngology at Sun Yat-sen University First Affiliated Hospital. This study received approval from the Ethics Committee of The First Affiliated Hospital of Sun Yat-sen University (Number: [2020]302). All enrolled patients were adults who provided written informed consent prior to enrollment. Peripheral blood and nasal tissue samples were collected from enrolled patients during their hospitalization for nasal endoscopic surgery. The study cohort included healthy controls (n=15), patients with chronic rhinosinusitis without nasal polyps (CRSsNP, n=18), and patients with chronic rhinosinusitis with nasal polyps (CRSwNP, n=62). Healthy controls comprised individuals undergoing septoplasty without sinusitis; mucosa from the inferior turbinate was collected during surgery. For CRSsNP and CRSwNP patients, sinus mucosa and nasal polyp tissues were collected during surgery, respectively. The exclusion criteria were as follows: 1) antibiotic use within 1 month prior to surgery; 2) use of systemic or topical corticosteroids; 3) diagnosis of severe autoimmune diseases, cystic fibrosis, primary ciliary dyskinesia, or acute respiratory infection. Post-excision, tissues were processed as follows: one portion was snap-frozen in liquid nitrogen and transferred to a -80°C freezer for storage, while another portion was fixed in 4% paraformaldehyde at 4°C for subsequent paraffin sectioning. Samples for bulk-tissue RNA sequencing, immunohistochemistry, and immunofluorescence analyses were derived from this cohort of enrolled patients. Detailed demographical and clinical information of all subjects is provided as Table S1.

Table S1. Demographical and clinical information of all subjects.

	HC	CRSsNP	CRSwNP
Subject number	15	18	62
Tissue type	inferior turbinate	sinus mucosa	nasal polyp
Male,n	11	13	45
Age(years), mean±SD	39.31±13.86	41.17±16.63	46.1±15.84
Patients with atopy, n	-	-	9
Patients with asthma, n	-	1	9
Recurrence,n	-	2	29

HC: healthy control; CRSsNP: chronic rhinosinusitis without nasal polyps; CRSwNP: chronic rhinosinusitis with nasal polyps.

Table S2. Identification of proteins demonstrating causal associations with NP.

Exposure	Outcome	eQTL				pQTL			
		Method	SNP	OR (95% CI)	FDR	Method	SNP	OR (95% CI)	FDR
QPCTL	Nasal polyps	IVW	2	0.51 (0.38-0.68)	4.87E-04	IVW	5	0.82 (0.74-0.91)	2.24E-02
LEAP2	Nasal polyps	IVW	4	0.51 (0.36-0.71)	4.50E-03	IVW	4	0.81 (0.72-0.90)	2.23E-02
IL2RB	Nasal polyps	IVW	4	2.95 (1.56-5.60)	2.14E-02	Wald ratio	1	0.39 (0.29-0.54)	9.49E-06
GLB1	Nasal polyps	IVW	13	0.80 (0.71-0.90)	1.04E-02	Wald ratio	1	0.22 (0.11-0.47)	1.57E-02
CTSS	Nasal polyps	IVW	27	1.35 (1.26-1.44)	3.07E-11	IVW	3	1.29 (1.17-1.43)	1.87E-04
B3GALT6	Nasal polyps	IVW	13	0.85 (0.81-0.91)	2.15E-05	Wald ratio	1	0.21 (0.12-0.38)	1.81E-04

SNP, single nucleotide polymorphism; OR, odds ratio; CI, confidence interval; IVW, inverse variance weighted.

Table S3. MR results of CTSS and QPCTL.

Exposure	Outcome	Cochran's Q test for heterogeneity					
		eQTL			pQTL		
		Q	Q_df	P value	Q	Q_df	P value
CTSS	Nasal polyps	36.885	26	0.077	0.842	2	0.656
QPCTL	Nasal polyps	0.005	1	0.941	2.466	4	0.651
		MR-Egger regression for directional pleiotropy					
		eQTL			pQTL		
		Intercept	SE	P value	Intercept	SE	P value
CTSS	Nasal polyps	0.001	0.013	0.967	0.011	0.032	0.795
QPCTL	Nasal polyps	NA	NA	NA	0.020	0.022	0.417
		MR-PRESSO Global test					
		eQTL			pQTL		
		RSSobs		P value			
CTSS	Nasal polyps	39.096		0.137	NA		NA
QPCTL	Nasal polyps	NA		NA	39.430		0.400

MR-PRESSO, Mendelian randomized pleiotropy residual sum and outlier; Q, Cochran's Q statistic; df, degrees of freedom; SE, standard error; RSSobs, observed residual sum of squares. NA indicated not enough single-nucleotide polymorphisms for analysis.

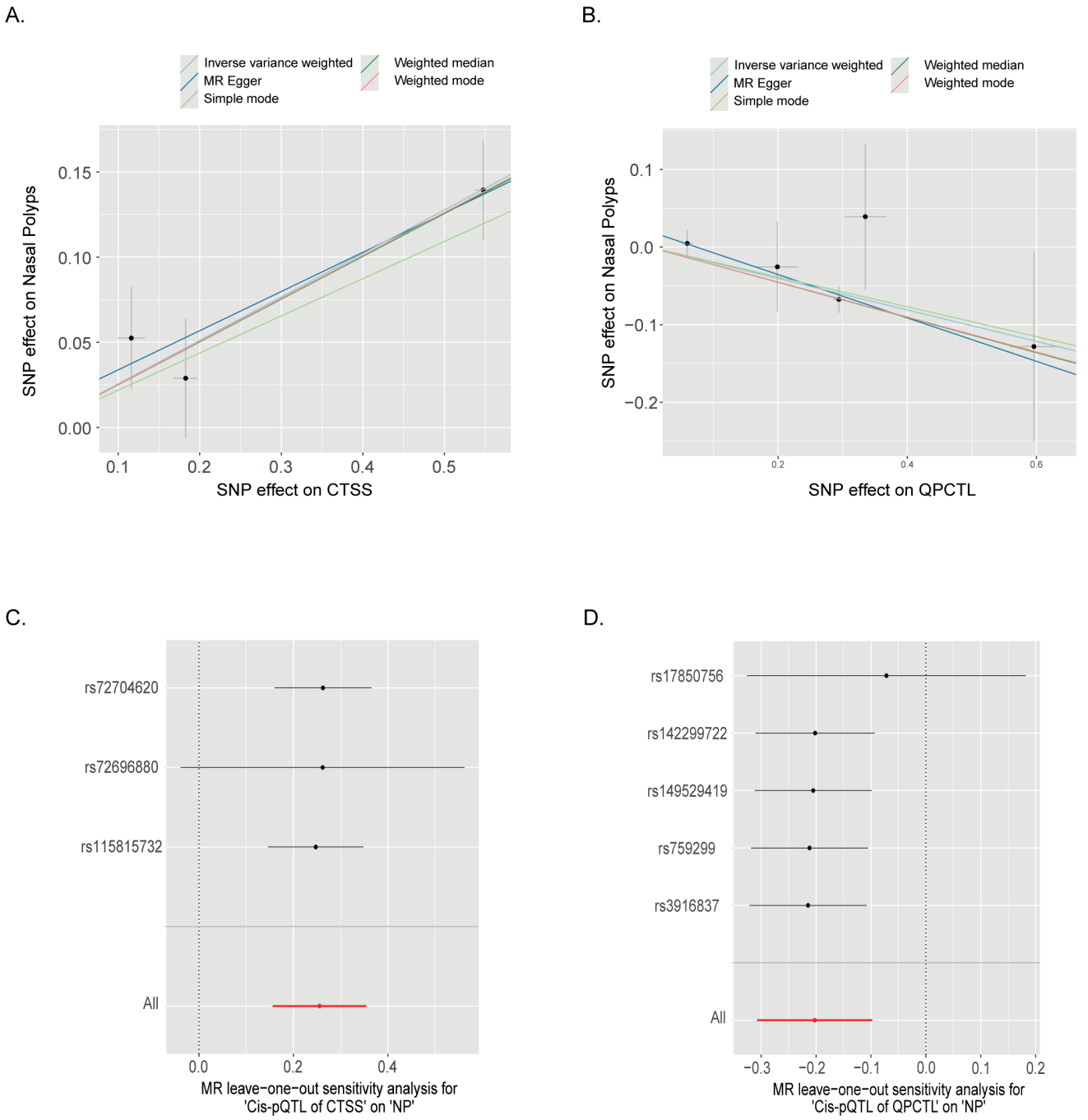

Figure S1. Scatterplot (A-B) and leave-one-out plot (C-D) for causal effect of CTSS and QPCTL proteins (Cis-pQTL) on the risk of nasal polyps.